AD-A170 709 LIGHT SCATTERING FROM SOLUTIONS OF ORGANOSILANE POLYMERS(U) IBM ALMADEN RESEARCH CENTER SAN JOSE CA P M COTTS ET AL. 07 AUG 86 TR-7 N00014-85-C-0056 1/1

UNCLASSIFIED F/G 7/3 NL

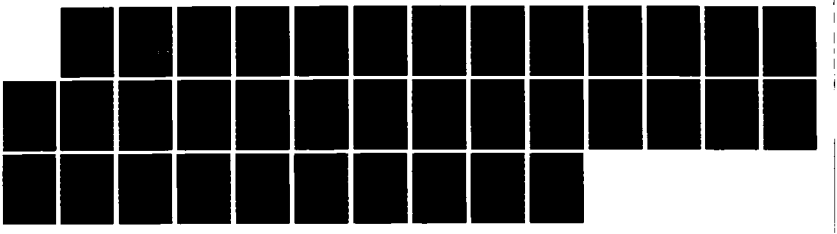

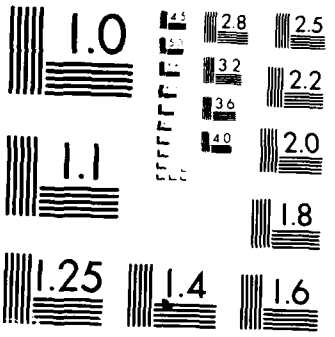

MICROCOPY RESOLUTION TEST CHART
NATIONAL BUREAU OF STANDARDS 1963-A

AD-A170 709

OFFICE OF NAVAL RESEARCH
CONTRACT N0014-85-C-0056
TASK NO. 631-850

"LIGHT SCATTERING FROM SOLUTIONS OF ORGANOSILANE POLYMERS"

by
P. M. COTTS, R. D. MILLER, P. T. TREFONAS III,
R. WEST AND G. N. FICKES

Submitted To Macromolecules

IBM Almaden Research Laboratory
650 Harry Road
San Jose, CA 95120-6099
August 7, 1986

DTIC FILE COPY

DTIC ELECTE AUG 7 1986 B

Reproduction in whole or in part is permitted for any purpose by the United States Government.
This document has been approved for public release and sale; its distribution is unlimited.

86 8 0 042

AD-A170 209

SECURITY CLASSIFICATION OF THIS PAGE

REPORT DOCUMENTATION PAGE

1a REPORT SECURITY CLASSIFICATION	1b RESTRICTIVE MARKINGS
2a. SECURITY CLASSIFICATION AUTHORITY UNCLASSIFIED	3 DISTRIBUTION/AVAILABILITY OF REPORT DISTRIBUTION STATEMENT A Approved for public release; Distribution Unlimited
2b. DECLASSIFICATION/DOWNGRADING SCHEDULE	
4. PERFORMING ORGANIZATION REPORT NUMBER(S) TECHNICAL REPORT NO. 7	5. MONITORING ORGANIZATION REPORT NUMBER(S)
6a. NAME OF PERFORMING ORGANIZATION IBM RESEARCH 6b. OFFICE SYMBOL (If applicable)	7a. NAME OF MONITORING ORGANIZATION ONR
6c. ADDRESS (City, State, and ZIP Code) IBM ALMADEN RESEARCH LABORATORY 650 HARRY ROAD SAN JOSE, CA. 95120-6099	7b. ADDRESS (City, State, and ZIP Code) OFFICE OF NAVAL RESEARCH CHEMISTRY ARLINGTON, VA. 22217
8a. NAME OF FUNDING/SPONSORING ORGANIZATION ONR 8b. OFFICE SYMBOL (If applicable)	9. PROCUREMENT INSTRUMENT IDENTIFICATION NUMBER
8c. ADDRESS (City, State, and ZIP Code) OFFICE OF NAVAL RESEARCH (CHEMISTRY) 800 N. QUINCY STREET ARLINGTON, VA. 22217	10 SOURCE OF FUNDING NUMBERS PROGRAM ELEMENT NO. C-0056 / PROJECT NO / TASK NO. / WORK UNIT ACCESSION NO
11 TITLE (Include Security Classification) LIGHT SCATTERING FROM SOLUTIONS OF ORGANOSILANE POLYMERS	
12 PERSONAL AUTHOR(S) P.M. COTTS, R. D. MILLER, P. T. TREFONAS III, R. WEST, G. N. FICKES	
13a. TYPE OF REPORT PUBLICATION 13b. TIME COVERED FROM ____ TO ____	14. DATE OF REPORT (Year, Month, Day) ~~7 17~~ 86 AUG. 7 15. PAGE COUNT 29
16. SUPPLEMENTARY NOTATION SUBMITTED TO MACROMOLECULES	

17 COSATI CODES			18 SUBJECT TERMS (Continue on reverse if necessary and identify by block number)
FIELD	GROUP	SUB-GROUP	POLYSILANE LIGHT SCATTERING, DIMENSIONS IN SOLUTION, MOLECULAR RIGIDITY

19 ABSTRACT (Continue on reverse if necessary and identify by block number)

ABSTRACT:A variety of high molecular weight organosilane polymers have recently been synthesized via the condensation of silyl dichlorides with sodium. These materials have applications as precursors to silicon carbide fibers and as positive resists for ultraviolet lithography. Light scattering results are presented which demonstrate that high molecular weight (10^6) and correspondingly large molecular dimensions (100 nm) in dilute solution are attainable. Relations among various molecular parameters obtained by static and dynamic light scattering are presented and discussed for varying substituents. The ratio of thermodynamic and hydrodynamic dimensions is compared with those reported for carbon backbone polymers where rotation is less hindered.

20 DISTRIBUTION/AVAILABILITY OF ABSTRACT ☐ UNCLASSIFIED/UNLIMITED ☐ SAME AS RPT ☐ DTIC USERS	21. ABSTRACT SECURITY CLASSIFICATION
22a NAME OF RESPONSIBLE INDIVIDUAL	22b TELEPHONE (Include Area Code) / 22c. OFFICE SYMBOL

LIGHT SCATTERING FROM SOLUTIONS OF ORGANOSILANE POLYMERS

P. M. Cotts
R. D. Miller

IBM Almaden Research Center
650 Harry Road
San Jose, California 95120-6099

P. T. Trefonas III
R. West

University of Wisconsin
Madison, Wisconsin

G. Fickes

University of Nevada
Reno, Nevada

ABSTRACT: Preliminary light scattering measurements have been carried out on the organopolysilanes (n-propylMeSi)$_n$, (PhMeSi)$_n$, (cyclohexylMeSi)$_n$, (n-octyl$_2$Si)$_n$ and (n-hexyl$_2$Si)$_n$. For the latter two samples measurements were carried out at various molecular weights. Very high molecular weights (10^6) and correspondingly large molecular dimensions (100 nm) in dilute solution may be observed for these polymers. Chain dimensions (R_G and R_H) together with molecular weights from light scattering indicate that the polysilanes are substantially more extended than carbon backbone polymers of similar degrees of polymerization. Hydrodynamic properties were determined in hexane by dynamic light scattering and viscometry for (n-hexyl$_2$Si)$_n$, which behaves as a flexible coil in this solvent.

Accession For
NTIS ☑
DTIC ☐
Unannounced ☐
Justification PER CALL FC
By
Distribution
Availability
Dist
A-1

LIGHT SCATTERING FROM SOLUTIONS OF ORGANOSILANE POLYMERS

P. M. Cotts
R. D. Miller

IBM Almaden Research Center
650 Harry Road
San Jose, California 95120-6099

P. T. Trefonas III
R. West

University of Wisconsin
Madison, Wisconsin

G. Fickes

University of Nevada
Reno, Nevada

ABSTRACT: Preliminary light scattering measurements have been carried out on the organopolysilanes $(\text{n-propylMeSi})_n$, $(\text{PhMeSi})_n$, $(\text{cyclohexylMeSi})_n$, $(\text{n-octyl}_2\text{Si})_n$ and $(\text{n-hexyl}_2\text{Si})_n$. For the latter two samples measurements were carried out at various molecular weights. Very high molecular weights (10^6) and correspondingly large molecular dimensions (100 nm) in dilute solution may be observed for these polymers. Chain dimensions (R_G and R_H) together with molecular weights from light scattering indicate that the polysilanes are substantially more extended than carbon backbone polymers of similar degrees of polymerization. Hydrodynamic properties were determined in hexane by dynamic light scattering and viscometry for $(\text{n-hexyl}_2\text{Si})_n$, which behaves as a flexible coil in this solvent.

I. INTRODUCTION

Substituted silane high polymers[1] represent a new class of radiation sensitive materials for which a number of recent applications have been discovered. In this regard, these materials have been utilized both as thermal precursors to silicon carbide[2] as photoinitiators in vinyl polymerizations,[3] and in photoresist applications.[4] The electronic spectra of polysilane derivatives are very unusual in that they absorb strongly in the UV in spite of the fact that the backbone is comprised solely of saturated sigma links. This absorption, which depends both on the substituents and the molecular weight,[5] has been described variously as a $\sigma\sigma^*$ or σ Si^{3d} transition.[6] Since there is considerable sigma delocation in the backbone, the electronic absorption should be dependent on the backbone conformation[7] and recent studies both in the solid state[8] and in solution suggest[9,10] that this is the case.

The presence of two large aliphatic and/or aromatic groups on each atom of the all Si backbone produces a chain with highly hindered rotational freedom about the backbone Si-Si bonds. The variation in rotational freedom with substituent is reflected both in the glass transition temperature, T_g, and in the wavelength of maximum ultraviolet absorption, λ_{max}. Parameters which reflect the overall molecular dimensions such as the root mean square radius of gyration R_G, and the hydrodynamic radius R_H are also expected to be larger than observed for carbon backbone polymers of similar degree of polymerization due to the rigidity arising from the hindrance to rotation. Static light scattering measurements of five polysilanes with varying substituents were used to determine the weight average molecular weight, M_w, the root mean square z-averaged radius of gyration, $R_{G,Z}$ and the second virial coefficient A_2. These parameters were used with information about the molecular weight distribution from size exclusion

chromatography to estimate the unperturbed dimensions, $R^2_{G,0}$ for a series of substituents. Two samples, poly(di-n-octylsilane) (hereafter abbreviated $(\text{n-octyl}_2\text{Si})_n$) and poly(di-n-hexylsilane) ($(\text{n-hexyl}_2\text{Si})_n$), were selected for more detailed study. The molecular weight dependence of R_G was investigated by permitting the photolytic degradation of these samples by room light. Hydrodynamic properties of $(\text{n-hexyl}_2\text{Si})_n$ were determined in hexane using dynamic light scattering and viscometry.

II. EXPERIMENTAL

A. Static Light Scattering

Static light scattering measurements were accomplished with three light scattering instruments: (1) SOFICA Model 42000 photogoniometer (University of Wisconsin), (2) Chromatix (LDC Milton Roy) KMX-6 low angle light scattering photometer (IBM), and (3) Brookhaven BI-200 SM photogoniometer (IBM). Measurements with the SOFICA were done with 546 nm light from a Hg vapor lamp at ambient temperature. Measurements with the KMX-6 and Brookhaven instruments were done with 632.8 nm light from He-Ne lasers (Melles Griot LHP121 and Spectra-Physics 124B, respectively) at 25.0 ± 0.2°C.

Differential refractive index increments (dn/dc) at 546.1 nm and 632.8 nm were measured using a Brice Phoenix differential refractometer (University of Wisconsin) or a Chromatix (LDC Milton Roy) KMX-16 differential refractometer (IBM), respectively. The results for all polymer solvent samples measured are in Table 1. The Brice Phoenix instrument was calibrated using aqueous sucrose solutions (dn/dc=0.00143 at 546.1 nm at 23°C)[11] and the KMX-16 was calibrated with aqueous sodium chloride solutions (dn/dc=0.174 at 632.8 nm and 25.0°C).[12] The parameters M_w, $R_{G,Z}$ and A_2 were determined by extrapolation of Kc/R_θ to $\theta=0$ and $c=0$ as is indicated by the relation

$$\frac{Kc}{R_\theta} = \frac{1}{M_w}\left(1 + 2A_2c + 3A_3c^2 + \ldots\right)\left(1 + \frac{q^2R_{G,Z}^2}{3} + \ldots\right) \qquad (1)$$

with

$$K = \frac{4\pi^2n^2(dn/dc)^2}{N_A\lambda_0^4}$$

and

$$q = \frac{4\pi n}{\lambda_0}\sin(\theta/2) \ .$$

R_θ is the Rayleigh factor measured at scattering angle θ, c is the concentration in g/mℓ, n is the refractive index of the solution, N_A is Avogadro's number, and λ_0 is the wavelength of the incident light in vacuum.

Simultaneous extrapolation of Kc/R_θ to zero scattering angle and infinite dilution were accomplished using a Zimm plot[11] as shown in Figure 1 for $(cyclohexylMeSi)_n$. For the very high molecular weight samples, the intramolecular interference factor, $P(\theta)$, can no longer be expressed in its linear limiting form used in Eq. 1 above:

$$P(\theta) = 1 - \frac{q^2R_{G,Z}^2}{3} \ ,$$

which is valid for small values of $q^2R_{G,Z}^2$, and a plot of Kc/R_θ versus q^2 is expected to curve upward. However, experimental data on a high molecular weight sample of $(n\text{-hexyl}_2Si)_n$, such as that shown in Figure 2, demonstrate that Kc/R_θ is linearly

dependent on q^2 even at high scattering angles. This is due to the compensating effect of sample polydispersity, which, for the most probable distribution, leads to an expression for the average $P(\theta)$ which is linear in $q^2R_G^2$ as shown by Zimm:[13]

$$P(\theta)^{-1} = 1 + \frac{1}{2} < q^2R_G^2 > \quad .$$

The most probable distribution is a close approximation of the experimental distribution obtained for the high M sample of $(\text{n-hexyl}_2\text{Si})_n$ as shown in Figure 3. Determination of M_w and A_2 for the high molecular weight samples was accomplished using a square-root plot of $(Kc/R_\theta)^{1/2}$ versus c where the subscript 0 indicates extrapolation to zero scattering angle. Measurements with the KMX-6 at $\theta=4.4^\circ$ were equivalent to the extrapolated zero angle ones determined with the Brookhaven goniometer at $20^\circ<\theta<150^\circ$, as shown in Figure 4. The square root plot is suggested to minimize extrapolation errors for high molecular weight polymers in good solvents where higher order terms in the virial expansion may contribute to the concentration dependence.[14-16]

The depolarization ratio, ρ_v is given by

$$\rho_v \equiv \frac{R_{Hv}}{R_{Vv}}$$

where R_{Hv} and R_{Vv} are the limiting Rayleigh factors of the light scattered at zero angle from a vertically polarized source with horizontally and vertically polarized analysers, respectively. Values of ρ_v varied from 0.0017 to 0.0023 for solutions of $(\text{n-hexyl}_2\text{Si})_n$ in hexane, so that corrections due to optical anisotropy were negligible.

B. Dynamic Light Scattering

Dynamic light scattering was measured using the Brookhaven 200 SM photogoniometer equipped with a BI2030 128 channel correlator to measure the time correlation function C(t) which was analyzed using the method of cumulants:[17]

$$\ell n\left(\frac{C(t)}{B} - 1\right)^{1/2} = \ell nb^{1/2} - \Gamma t + \mu_2 t^2/2 + \ldots \qquad (2)$$

with B the baseline of the correlation function and b an optical constant. The diffusion coefficient D_c at each concentration c is obtained from the extrapolation of the reduced first cumulant, $\Gamma_{c,q}/q^2$, to zero scattering angle:

$$D_{z,c} = \lim_{q \to 0} (\Gamma_{c,q}/q^2) \ .$$

The normalized second cumulant, μ_2/Γ^2, which reduces to zero for a purely single exponential decay, describes the deviation from a single exponential arising from polydispersity or other relaxations. The sample time Δt was selected with the criterion

$$\Delta t = \frac{2}{m\Gamma}$$

with m the number of channels. We have used a measured baseline (average of four delay channels 1029 to 1032 times the sample time Δt) as B, however, the calculated baseline (infinite time value) and measured baseline agreed within 0.1% for all measurements used.

C. Viscometry and Size Exclusion Chromatography

The intrinsic viscosity, $[\eta]$ of poly(di-n-hexylsilane) in hexane was measured using a Cannon Ubbelohde semi-micro viscometer equipped with a Wescan automatic vicosity timer. $[\eta]$ was determined by extrapolation of the reduced viscosity, η_{sp}/c and the inherent viscosity, $\ln \eta_{rel}/c$ to infinite dilution, as shown in Figure 5, using the Huggins and Kramers relations:

$$\frac{\eta_{sp}}{c} = \frac{\eta_{rel} - 1}{c} = [\eta] + k[\eta]^2 c + ...$$

and

$$\frac{\ln \eta_{rel}}{c} = [\eta] - (1/2 - k)[\eta]^2 c + ...$$

with $\eta_{rel}=\eta/\eta_0$ with η and η_0 the viscosities of the solution and solvent, respectively. $[\eta] \equiv 474$ ml/g and the Huggins coefficient k was 0.357, similar to values usually observed for flexible polymers in good solvents. Although kinetic energy corrections are expected to be very small at these flow times, significant deviation from the limiting $[\eta]$ at zero shear rate may be possible at the high molecular weight used and this was not assessed.

Size exclusion chromatography was used to estimate the polydispersity of each sample. 150 $\mu\ell$ of each sample at a concentration of approximately 1 mg/mℓ was injected onto a set of four mixed gel columns (ASI Ultragel), using tetrahydrofuran (THF) as the mobile phase and a differential refractometer as the concentration detector. The column set was calibrated with a series of narrow distribution polystyrene standards (Polymer Laboratories) and a calibration curve was fit to a third order polynomial:

$$\log M = A + Bt + Ct^2 + Dt^3$$

where t is the peak elution time of a PS standard of molecular weight M. Calculation of apparent molecular weight averages relative to polystyrene, M_w^{PS}, M_n^{PS}, M_z^{PS} and the polydispersity (M_w^{PS}/M_n^{PS}) were carried out using an IBM PCXT with chromatography software (Nelson Analytical). An example of a typical distribution obtained is shown in Figure 3 for $(n\text{-hexyl}_2Si)_n$.

III. RESULTS AND DISCUSSION

A. Static Light Scattering

The molecular parameters obtained from static light scattering: M_w, $R_{G,Z}$ and A_2 are listed in Table 2 for the various polysilanes studied. The polydispersity, M_w/M_n, and the molecular weight relative to the polystyrene calibration, M_w^{PS}, obtained from size exclusion chromatography are also listed. It is apparent that very high molecular weights may be obtained for these polymers. The apparent molecular weights M_w^{PS} obtained by SEC cannot be directly compared with true weight average molecular weights determined by light scattering. For the very high molecular weight samples of $(n\text{-octyl}_2Si)_n$ and $(n\text{-hexyl}_2Si)_n$, the elution times of the samples approached the exclusion limit of the columns used, so that these values of M_w^{PS} are more uncertain. Due to the difficulty in synthesizing a range of molecular weights, the molecular weight dependence of R_G was investigated for $(n\text{-octyl}_2Si)_n$ and $(n\text{-hexyl}_2Si)_n$ by permitting photochemical degradation in room light. This degradation in M was sufficiently slow to permit measurement of M_w and R_G as the samples degraded, as shown in Figure 6. The exponent ν in the relation

$$R_G \propto M^{\nu}$$

is equal to 0.62 as is observed for flexible coil polymers in good solvents. Random chain scission is expected to lead to a normal distribution not substantially different from the original distribution of these samples, so that the exponent of 0.62 would also be expected for a series of narrow distribution samples. The exponent of 0.62 is direct evidence for the coil-like configuration of the polymer chain. The larger R_G obtained in hexane is consistent with the larger A_2 measured in this solvent and suggests that excluded volume effects are significant in spite of the highly hindered rotational freedom.

The linearity of the $P^{-1}(\theta)$ function for $0° < \theta < 150°$ permits the use of the KMX-6 to estimate R_G from measurements at only two angles, 4.4° and 175.6°, analogous to dissymmetry measurements used early in light scattering experiments. This technique requires experimental evidence for the linearity of the $P^{-1}(\theta)$ function such as that shown in Figure 2 since the presence of large scattering species such as dust or aggregates, or large polydispersity can introduce significant curvature which cannot be assessed with measurement at only two angles. The KMX-6 provides a degree of precision (±0.2%) which we have not been able to attain with the more traditional goniometer. Measurement of R_G using this"dissymmetry" method over a range of concentrations for $(\text{n-hexyl}_2\text{Si})_n$ in hexane showed a decrease in R_G with increasing concentration, as is shown in Figure 6. The decrease in R_G with increasing concentration in dilute solution due to competing intramolecular and intermolecular interactions has been predicted[18-21] and confirmed by neutron scattering measurements.[22] For light scattering, determination of R_G at a finite concentration c requires the assumption that the function $Q(\theta)$ representing the intermolecular interference in the more complete expression of Eq. (1)

$$\frac{K_c}{R_\theta} = \frac{1}{M_w P(\theta)} + 2\ A_2 Q(\theta) c + \ldots$$

is negligible, *i.e.*, $Q(\theta)$ is nearly unity. Since the observed decrease in R_G in Figure 7 is very similar to that observed by Jannink *et al.*[20] using neutron scattering, this assumption appears to be reasonable.

B. Dynamic Light Scattering

The linewidth Γ determined by the method of cumulants (Eq. (2), above) is shown as a function of q^2 for several concentrations of $(\text{n-hexyl}_2\text{Si})_n$ in hexane in Figure 8. The q^2 dependence is linear as expected for diffusive motion. Measurements were carried out at scattering angles θ=20, 30, 45, and 60°. Values of the normalized second cumulant μ_2/Γ^2 were 0.17±0.04, and were independent of angle and concentration in this range. In the low q region ($qR_G<1$) the magnitude of μ_2/Γ^2 reflects the polydispersity of the sample. The polydispersity determined from dynamic light scattering may be compared with that obtained from SEC, provided the exponent ν in the relation

$$D \propto M^{-\nu}$$

is known. Here we use ν=0.6 based on the measurements of R_G of photolytically degraded samples discussed above. Substitution of ν=0.6 and $\delta \equiv M_w/M_n - 1 = 1.3$ (see Table 2) into the expression[23]

$$\frac{\mu_2}{\Gamma^2} = \frac{\nu^2}{4} \frac{\delta[4 + (1-\nu)(\nu-5)\delta]}{[1 + [(2-\nu)(1-\nu)/2]\delta]^2}$$

yields μ_2/Γ^2=0.11 in reasonable agreement with the experimental value of 0.17±0.04 for $(\text{n-hexyl}_2\text{Si})_n$. Above 60° scattering angle ($qR_G>1$) the deviation from a single exponential became more significant indicating contributions from internal motions of

the chain. The concentration dependence of D_c is shown in Figure 9, and may be expressed as

$$D_c = D_0(1 + k_D c)$$

with $D_0 = 1.07 \times 10^{-7}$ cm^2/sec and $k_D = 287$ cm^3/g. The hydrodynamic radius, R_H, defined by the Einstein relation for a hard sphere

$$D_0 = \frac{kT}{6\pi\eta_0 R_H}$$

is 64 nm. The hard sphere value for A_2

$$A_2 = \frac{4N_A}{M_w^2} V_H$$

where V_H is the hydrodynamic volume of the sphere

$$V_H = \frac{4}{3} \pi R_H^3$$

may be compared with the experimental A_2. We obtain $10^4 A_2 = 0.71$ ml/g mole in good agreement with the experimental value of $10^4 A_2 = 0.76$ ml/g mole measured by static light scatttering for $(n\text{-hexyl}_2\text{Si})_n$ in hexane. This agreement suggests that the polymer coil behaves thermodynamically as well as hydrodynamically like a hard sphere of radius R_H. The concentration dependence k_D of the diffusion coefficient may also be expressed in volume fraction units

$$k_D^{\Phi} = \frac{M_w}{N_A V_H} k_D$$

which yields $k_D^{\Phi} = 2.7$ in reasonable agreement with the Yamakawa prediction of 2.2 for the good solvent limit.[24]

The ratio $R_G/R_H=1.69$ in good agreement with the prediction of 1.73 for polydisperse flexible coils with a most probable distribution.[25] R_H and R_G may be compared with a radius $R_{G,\eta}$ calculated from the intrinsic viscosity $[\eta]$ using the Fox-Flory equation:[26]

$$[\eta] = \frac{6^{3/2}\Phi R_{G,\eta}^3}{M_w}$$

where Φ is the Flory viscosity constant, 2.5×10^{23} for polydisperse samples with infinite hydrodynamic interaction. For $(\text{n-hexyl}_2\text{Si})_n$ in hexane, $[\eta]$=474 mℓ/g at 20°C, so that $R_{G,\eta}$=90 nm. The intrinsic viscosity $[\eta]$ measures an average which is close to a weight average, so that $R_{G,\eta}$ is expected to be smaller than $R_{G,Z}$ determined by light scattering by a factor which may be estimated to be 0.83 based on the SEC results for M_z/M_w. The experimental ratio, $R_{G,\eta}/R_{G,Z}$=0.83, in excellent agreement with the SEC results. The hydrodynamic radius R_H determined by dynamic light scattering may be compared directly with $R_{G,\eta}$, since both measurements yield an average which is close to a weight average. The ratio $R_{G,\eta}/R_H$=1.41, which is quite consistent with the value of 1.50 predicted for monodisperse chains in the nondraining limit (infinite hydrodynamic interaction). Although the first cumulant from dynamic light scattering on polydisperse molecules measures a z-average diffusion coefficient

$$< D >_z = \Sigma w_i M_i D_i / M_w$$

the inverse relation of D to M results in the hydrodynamic radius R_H being most closely related to that obtained for a monodisperse sample with the same M_w rather than M_z.

C. Estimation of Unperturbed Chain Dimensions

The light scattering data in Table 2 may be used to estimate the characteristic ratio, C_∞, or $(R^0_{G,W})^2/M_w$ which may be compared with values for other polymers to assess the flexibility of the chain. The superscript 0 indicates a measurement at θ conditions where excluded volume effects are absent, and the subscript w indicates a correction of the measured $R_{G,Z}$ to an average appropriate for comparison with M_w, *i.e.*, such that

$$\frac{(R^0_{G,W})^2}{M_w} \cong \frac{(R^0_G)^2}{M} \tag{3}$$

where the parameters on the right hand side of Eq. (3) are determined for a narrow distribution fraction. Since $R_G \propto M^{0.6}$

$$\frac{R_{G,Z}}{R_{G,W}} \propto \left(\frac{M_z}{M_w}\right)^{0.6} .$$

Correction of $R_{G,W}$ for expansion due to excluded volume requires estimate of the expansion factor

$$\alpha_s \equiv \frac{R_G}{R^0_G} .$$

This may be obtained from various approximate theories which relate α_s and the interpenetration function ψ where[16]

$$\psi = \frac{A_2 M_w^2}{4\pi^{3/2} N_A R_{G,w}^3} .$$

Experimental values of ψ are listed in Table 3, and are very large for the high molecular weight samples of $(\text{n-hexyl}_2\text{Si})_n$ and $(\text{n-octyl}_2\text{Si})_n$. Various theories predict an upper limit on ψ of 0.2-0.3 and experimentally, values larger than 0.3 are rarely observed for flexible chain polymers.[16] The limited number of samples and large values of ψ make estimation of the magnitude of the excluded volume effect very approximate. Use of the available theories for ψ and α_s, along with experimental data obtained for polystyrene and polychloroprene[14] lead to estimates of $\alpha_s \cong 1.3 \pm 0.3$ for $(\text{n-hexyl}_2\text{Si})_n$ in hexane. An empirical relation between the experimental parameter $A_2 M_w/[\eta]$ and α_s^2 -1 also leads to an estimate of ~1.3 for α_s for $(\text{n-hexyl}_2\text{Si})_n$ in hexane.[16] Using these expressions and the information about the polydispersity listed in Table 1 we obtain the values for $R_{G,w}^0$ and N_w shown in Table 3, where N_w is the weight average number of backbone chain atoms. The values of $(R_{G,w}^0)^2/N_w$ are 15-30 (with dimensions in Å), substantially larger than the values of 2-4 observed for typical carbon backbone polymers such as polystyrene, poly(methylmethacrylate), etc. The characteristic ratio, C_∞, where

$$C_\infty = \frac{\langle r^2 \rangle_0}{N\ell^2}$$

with $\langle r^2 \rangle_0$ the mean square end-to-end distance and l the length of the Si-Si bond, 2.35Å, may also be calculated. We assume that $\langle r^2 \rangle_0 \cong 6(R_{G,w}^0)^2$ as for Gaussian chains and obtain the values listed in Table 3. For the poly(di-n-hexylsilane), $C_\infty \cong 20$ which is larger than the value of 10 obtained for polystyrene for example.

Although C_∞ is substantially larger than is observed for carbon backbone polymers, the difference is not as large as is observed in the values of $(R^0_{G,w})^2/N_w$. The larger effect in the $(R^0_{G,w})^2/N_w$ parameter is due to the contribution from the longer Si-Si bond. The characteristic ratio reflects only the rigidity due to rotational hindrance and fixed valence angles. In the case of polymers containing aromatic groups in the backbone, equivalent "bond lengths" can be quite large, leading to very large valves of $(R^0_{G,w})^2/N_w$. However, rotation about these long bonds is often unhindered by steric constraints so that C_∞ would be small and suggest a high degree of flexibility. The values of $R^0_{G,w}$ and C_∞ obtained for the samples other than $(\text{n-hexyl}_2\text{Si})_n$ are less certain due to the limited measurements. In particular some samples contained a small high molecular weight fraction which can have a very large effect on $R_{G,z}$ measured by light scattering. The agreement among the measurements of the poly(di-n-hexylsilane) for the different solvents and instruments used, and the agreement with hydrodynamic measurements discussed above substantially improves the reliability of C_∞ for this sample, however as discussed above, estimation of the magnitude of the excluded volume effect is very uncertain. Measurements in a θ-solvent are required before a definitive conclusion about the flexibility of these polymers can be made.

Although it appears that the $(\text{n-hexyl}_2\text{Si})_n$ chain is quite flexible, at least by equilibrium measurements, we can estimate the persitence length ρ using the Kratky-Porod model.[28] Near the coil limit, ρ may be determined by solving simultaneous expressions for the contour length L and R^2_G in terms of equivalent Kuhn segments ℓ_k:

$$L = n\ell_k$$

$$R^2_G = \frac{1}{6}\, n\ell^2_k \,.$$

The contour length L is estimated as $N_w\ell$ where N_w is the number of backbone Si atoms and ℓ is the projection of the Si-Si bond onto the backbone, 1.94Å. The persistence length $\rho=\ell_k/2$. For $(\text{n-hexyl}_2\text{Si})_n$ we obtain ℓ_k=5.8 nm and ρ=2.9 nm, using the value of $R^0_{G,w}$ listed in Table 3. Use of experimentally determined $R_{G,z}$ from light scattering, without correction for polydispersity and excluded volume effects leads to a much larger estimate for the persistence length ρ. Although estimates for these corrections are uncertain, they are reinforced by agreement with hydrodynamic dimensions obtained with independent techniques.

Chain dimensions (R_G and R_H) and molecular weights obtained from light scattering indicate that the polysilanes are substantially more extended than carbon backbone polymers of similar degree of polymerization. This increase in size is due to the longer Si-Si bond length and to the highly substituted backbone which provides a large degree of steric hindrance to rotation. Despite the large dimensions, the chains appear to behave as flexible coils at the very high molecular weights studied. This is evidenced by the exponent of 0.62 in the relation of R_G to M, and by the decrease in R_G of the $(\text{n-hexyl}_2\text{Si})_n$ in the poorer solvent THF relative to the R_G obtained in hexane. The question of whether or not the chains obey Gaussian statistics with an exponent of 0.5 in a θ-solvent where excluded volume effects are absent awaits measurements in a θ-solvent. The temperature dependence of the overall chain dimensions, which has been suggested undergoes a low temperature transition,[9,10] is also being investigated.[29]

ACKNOWLEDGMENT

R. D. Miller gratefully acknowledges partial financial support by the Office of Naval Research.

Table 1

Differential Refractive Index Increments

Polymer	Solvent	λ(nm)	T(°C)	dn/dc (mℓ/g)
$(n\text{-PrMeSi})_n$	THF	546.1	22.3[a]	0.200
$(cyclohexylMeSi)_n$	cyclohexane	546.1	22.3[a]	0.167
$(n\text{-hexyl}_2Si)_n$	THF	546.1	22.3[a]	0.106
$(n\text{-hexyl}_2Si)_n$	THF	632.8	25.0°[a]	0.085_5
$(n\text{-hexyl}_2Si)_n$	hexane	632.8	25.0[b]	0.121_4
$(n\text{-octyl}_2Si)_n$	THF	632.8	25.0[b]	0.119
$(MePhSi)_n$	THF	632.8	25.0[b]	0.296

[a] ±0.5°C.
[b] ±0.2°C.

Table 2

Molecular Parameters of Organosilane Polymers

Sample	Solvent	M_w^{LS}	10^4A_2	R_G(nm)	M_w/M_n	M_w^{PS}
$(n\text{-PrMeSi})_n$	THF	210,000	2.18	31	3.1	180,000
$(cyclohexylMeSi)_n$	cyclohexane	2,540,000	1.24	76	2.7	800,000
$(n\text{-hexyl}_2Si)_n$	cyclohexane	7,400,000	0.47	102	1.3	2,200,000
$(n\text{-hexyl}_2Si)_n$	hexane	6,100,000	0.76	108	2.3	1,900,000
$(n\text{-hexyl}_2Si)_n$	THF	6,300,000	0.43	92	2.3	1,900,000
$(n\text{-octyl}_2Si)_n$	THF	3,200,000	0.98	100	2.4	2,600,000
$(MePhSi)_n$	THF	46,000	3.6	21	4.2	19,000

Table 3

Estimation of Unperturbed Dimensions

Sample	N_w	Solvent	ψ	$R^0_{G,w}$(nm)	C_∞
$(n\text{-PrMeSi})_n^*$	2470	THF	0.07	21	19
$(cyclohexylMeSi)_n$	20188	cyclohexane	0.14	50	14
$(n\text{-hexyl}_2Si)_n$	37373	cyclohexane	0.25	87	21
$(n\text{-hexyl}_2Si)_n$	31313	hexane	0.30	77	20
$(n\text{-hexyl}_2Si)_n$	31313	THF	0.20	76	20
$(n\text{-octyl}_2Si)_n$	12598	THF	0.18	59	30
$(MePhSi)_n^*$	383	THF	0.02	15	64

*These showed a small secondary peak in the SEC chromatogram in the high M region.

REFERENCES

1. (a) For reviews of polysilanes, see R. West, *J. Organometallic Chem.* **300**, 327 (1986); (b) R. West: "Organopolysilanes," in Comprehensive Organometallic Chemistry, E. Abel (ed.) Perganon Press Ltd. Oxford, England, 1982, Ch. 9.4, pp. 365-397.
2. (a) S. Yajima, Y. Hasegawa, Y. Hayaski, M. Imura, *J. Mat. Sci.* **13**, 2569 (1975); (b) Y. Hasegawa, M. Imura, S. Yajima, *J. Mat. Sci.* **15**, 2569 (1978).
3. R. West, A. R. Wolff and D. J. Peterson, *J. Radiat. Curing* **13**, 35 (1986); A. R. Wolff and R. West, *Applied Organomet. Chem.*, in press.
4. (a) R. D. Miller, D. Hofer, D. R. McKean, C. G. Willson, R. West and P. Trefonas III, in Materials for Microlithography, C. G. Willson and J. M. J. Frèchet, Eds., ACS Symposium Series No. 266 American Chemical Society, Washington, D. C., 1984; (b) D. C. Hofer, R. D. Miller and C. G. Willson, Proceedings SPIE Adv. Resist Technol. **469**, 108 (1984); (c) D. C. Hofer, R. D. Miller and C. G. Willson, ibid., 16.
5. P. Trefonas III, R. West, R. D. Miller and D. Hofer, *J. Polym. Sci., Polym. Lett. Ed.* **21**, 823 (1983).
6. C. G. Pitt, in "Homoatomic Rings, Chains and Macromolecules of the Main Group Elements," A. L. Rheingold, Ed., Elsevier Publ., New York, 1977.
7. H. Bock, W. Ensslin, F. Féher and R. Freund, *J. Am. Chem. Soc.* **98**, 668 (1976).
8. R. D. Miller, D. Hofer, J. F. Rabolt and G. N. Fickes, *J. Am. Chem. Soc.* **107**, 2172 (1985).
9. P. Trefonas III, J. R. Damewood, Jr., R. West and R. D. Miller, *Organometallics* **4**, 1318 (1985).
10. L. A. Harrah and J. M. Ziegler, *J. Polym. Sci., Polym. Lett. Ed* **23**, 209 (1985).
11. Maron and Lou, *J. Phys. Chem.* **59**, 231 (1955).
12. A. Kruis, *Z. Physik. Chec* **B34**, 13 (1936).
13. B. H. Zimm, *J. Chem. Phys* **16**, 1093 (1948); **16**, 1099 (1948).

14. P. J. Flory, "Principles of Polymer Chemistry," Cornell University Press, Ithaca, New York 1953, Ch. VII.

15. G. C. Berry, *J. Chem. Phys.* **44**, 4550 (1966).

16. H. Yamakawa, "Modern Theory of Polymer Solutions," Harper and Row, New York, 1971, Ch. VII.

17. D. E. Koppel, *J. Chem. Phys.* **57**, 4814 (1972).

18. M. Fixman and J. M. Peterson, *JACS* **86**, 3524 (1969).

19. W. Graessley, *Polymer* **21**, 258 (1980).

20. I. C. Sanchez and D. J. Lohse, *Macromolecules* **14**, 131 (1981).

21. A. Z. Akcasu and B. Hammouda, *Macromolecules* **16**, 951 (1983).

22. G. Jannink, *et al.*, *Macromolecules* **8**, 804 (1975).

23. J. Selser, *Macromolecules* **12**, 909 (1979).

24. H. Yamakawa, *J. Chem. Phys.* **36**, 2995 (1962).

25. I. Frenker and W. Burchard, *Macromolecules* **6**, 848 (1973).

26. P. J. Flory and T. G. Fox, Jr., *J. Am. Chem. Soc.* **73**, 1904 (1951).

27. P. J. Flory, "Statistical Mechanics of Chain Molecules," Wiley Interscience, New York, 1969, Ch. I.

28. O. Kratky and G. Porod, *Rec. Trav. Chim.* **68**, 1106 (1949).

29. P. M. Cotts, Proceedings of Polymeric Materials, Science and Engineering Division, ACS **53**, 336 (1985).

FIGURE CAPTIONS

Figure 1. Zimm plot of the elastic light scattering from solutions of (cyclohexylMeSi)$_n$ in cyclohexane at 23°C obtained with the SOFICA. Circles are experimental data and squares are the values obtained by extrapolation to zero angle or zero concentration.

Figure 2. Angular dependence of the elastic light scattering from solutions of (n-hexyl$_2$Si)$_n$ in hexane at 25° obtained with the Brookhaven goniometer from 20° to 150° scattering angle.

Figure 3. Comparison of the experimental chromatogram obtained for (n-octyl$_2$Si)$_n$ in THF with SEC (solid line) with the calculated most probable (Zimm-Schulz) distribution (dashed line).

Figure 4. Concentration dependence of the zero angle elastic scattering from solutions of (n-hexyl$_2$Si)$_n$ in hexane and THF at 25°C.

Figure 5. The reduced viscosity, η_{sp}/c, and the inherent viscosity, ln η_{rel}/c, as a function of concentration for (n-hexyl$_2$Si)$_n$ in hexane at 20°C.

Figure 6. The dependence of the root mean square radius of gyration from light scattering, R_G^{LS}, on M_w for series of (n-hexyl$_2$Si)$_n$ and (n-octyl$_2$Si)$_n$ obtained by photolytic degradation in THF and hexane.

Figure 7. The decrease in $R_G^{LS,APP}$ with concentration for (n-hexyl$_2$Si)$_n$ in hexane.

Figure 8. The linewidth Γ obtained from cumulant analysis of dynamic light scattering as a function of scattering angle for four concentrations of $(\text{n-hexyl}_2\text{Si})_n$ in hexane at 25°C.

Figure 9. The concentration dependence of Γ_c obtained from extrapolation of Γ to zero angle for $(\text{n-hexyl}_2\text{Si})_n$ in hexane.

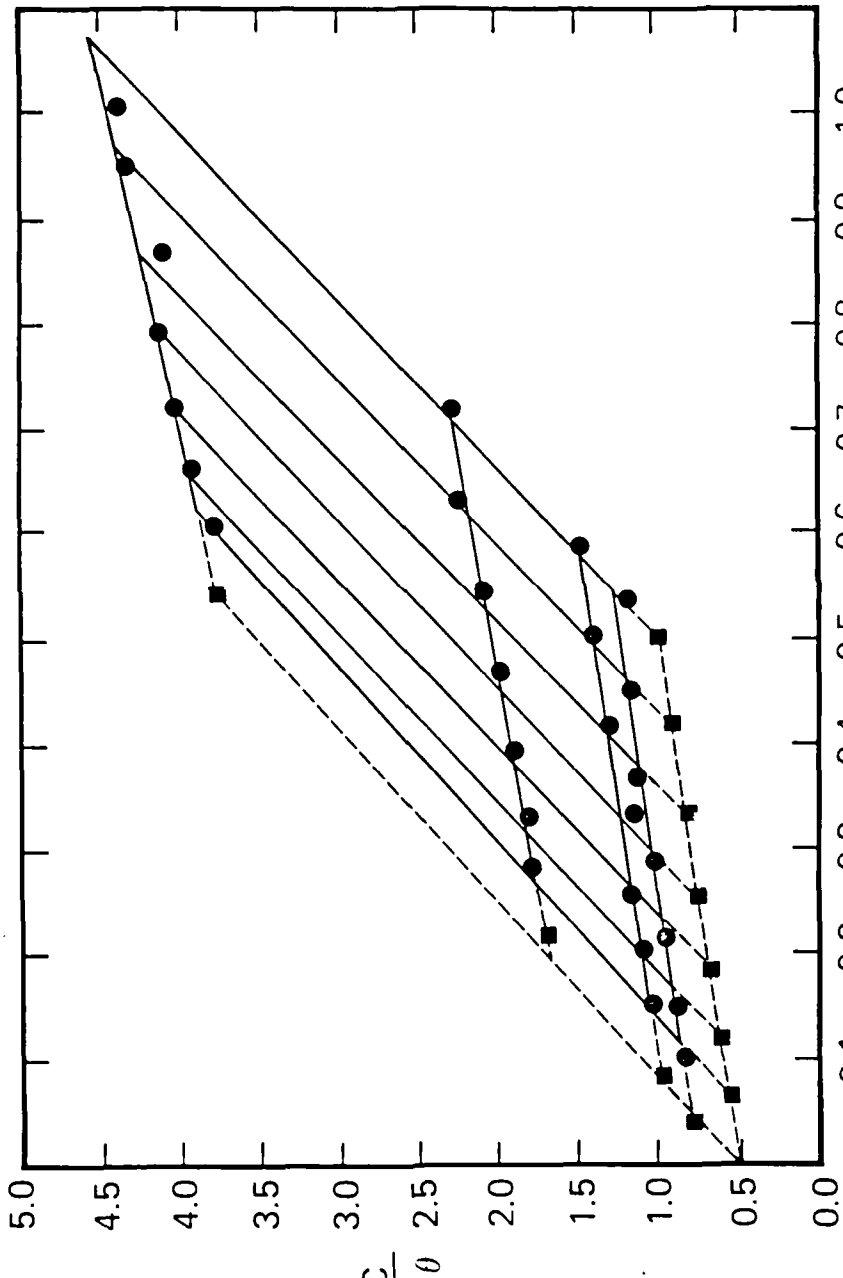

Figure 1. Zimm plot of the elastic light scattering from solutions of $(cyclohexylMeSi)_n$ in cyclohexane at 23 °C obtained with the SOFICA. Circles are experimental data and squares are the values obtained by extrapolation to zero angle or zero concentration.

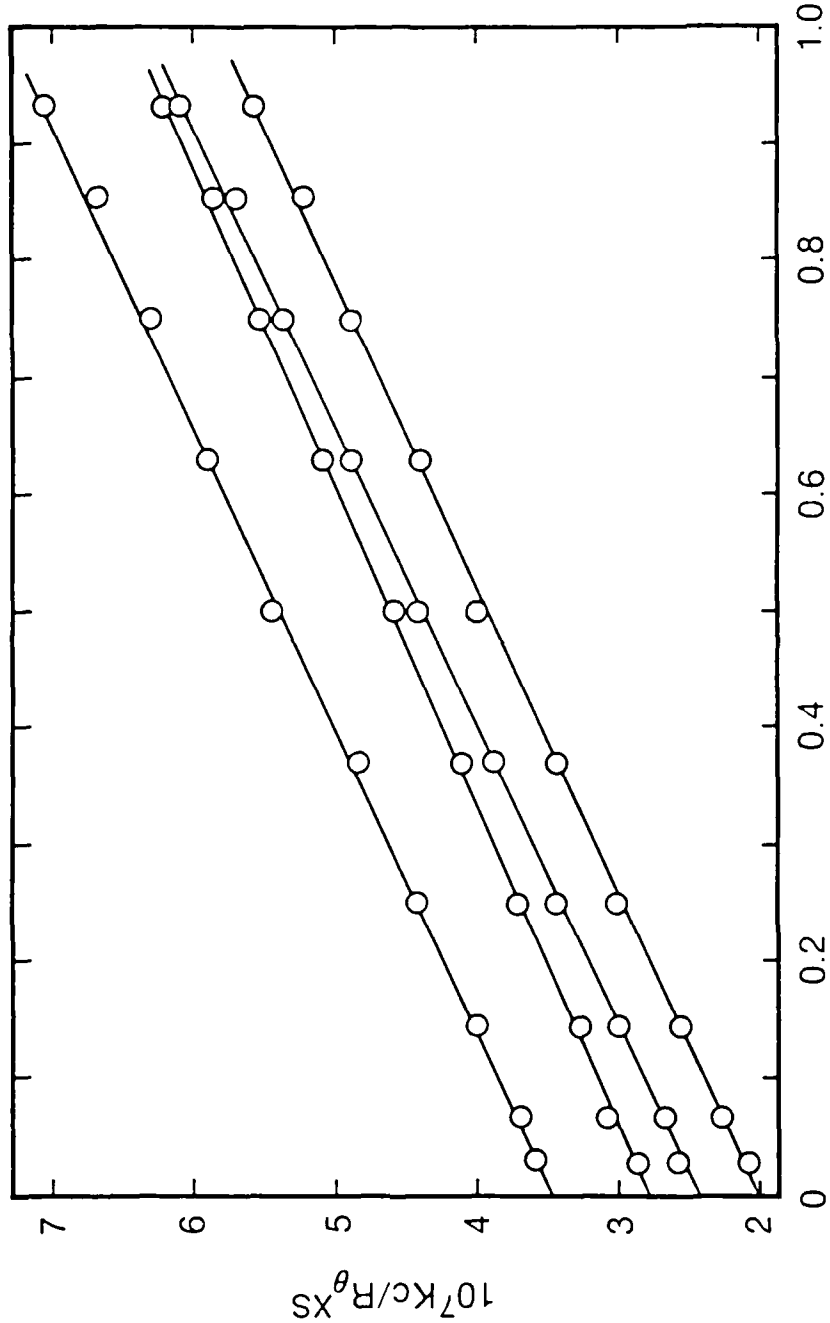

Figure 2. Angular dependence of the elastic light scattering from solutions of $(n\text{-hexyl}_2Si)_n$ in hexane at 25° obtained with the Brookhaven goniometer from 20° to 150° scattering angle.

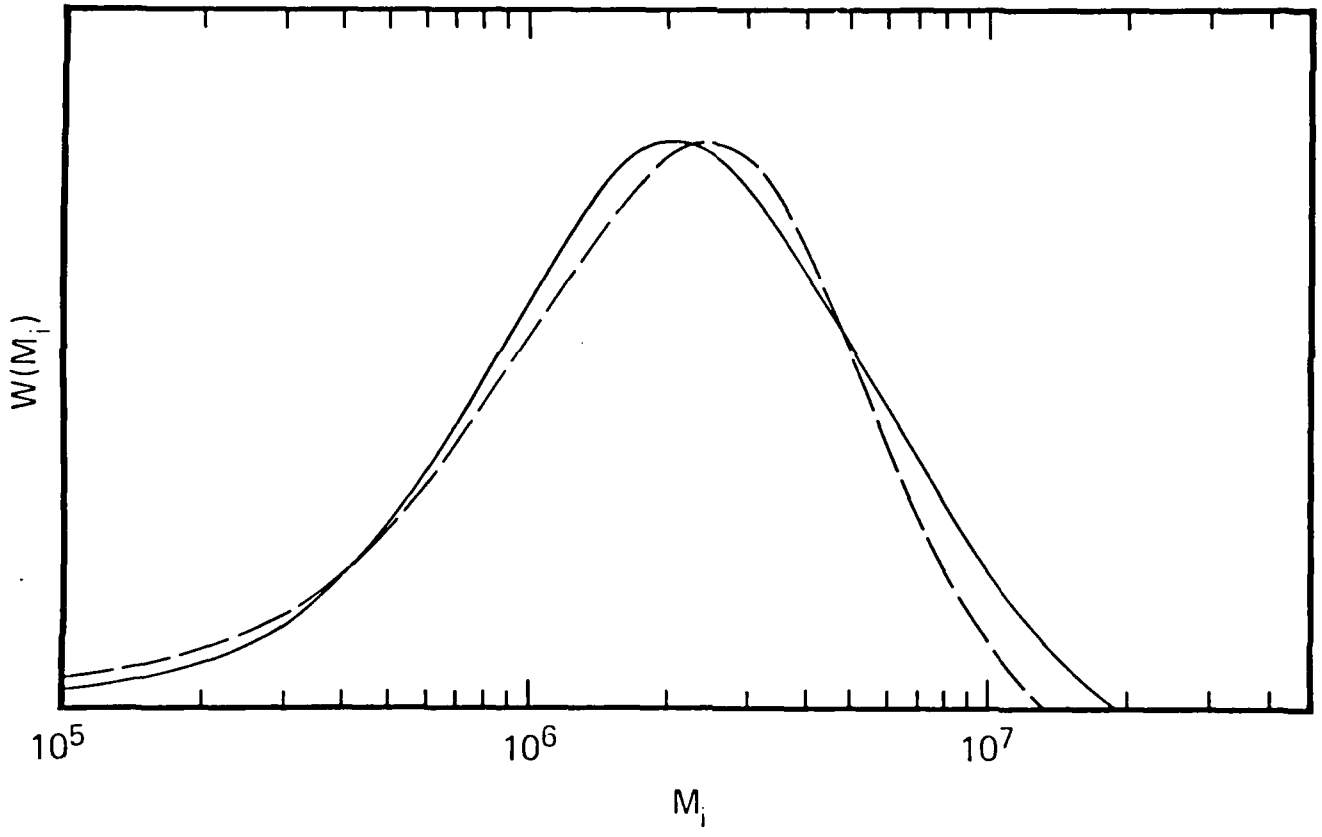

Figure 3. Comparison of the experimental chromatogram obtained for (n-octyl$_2$Si)$_n$ in THF with SEC (solid line) with the calculated most probable (Zimm-Schulz) distribution (dashed line).

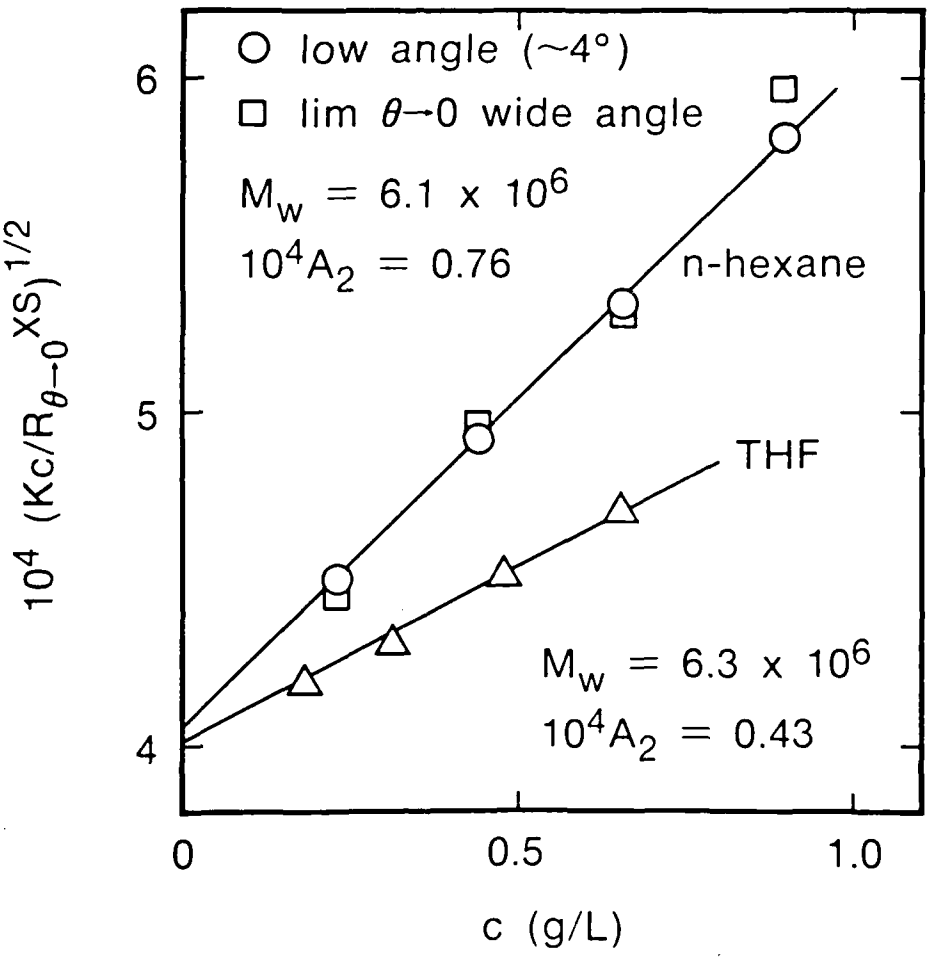

Figure 4. Concentration dependence of the zero angle elastic scattering from solutions of $(\text{n-hexyl}_2\text{Si})_n$ in hexane and THF at 25°C.

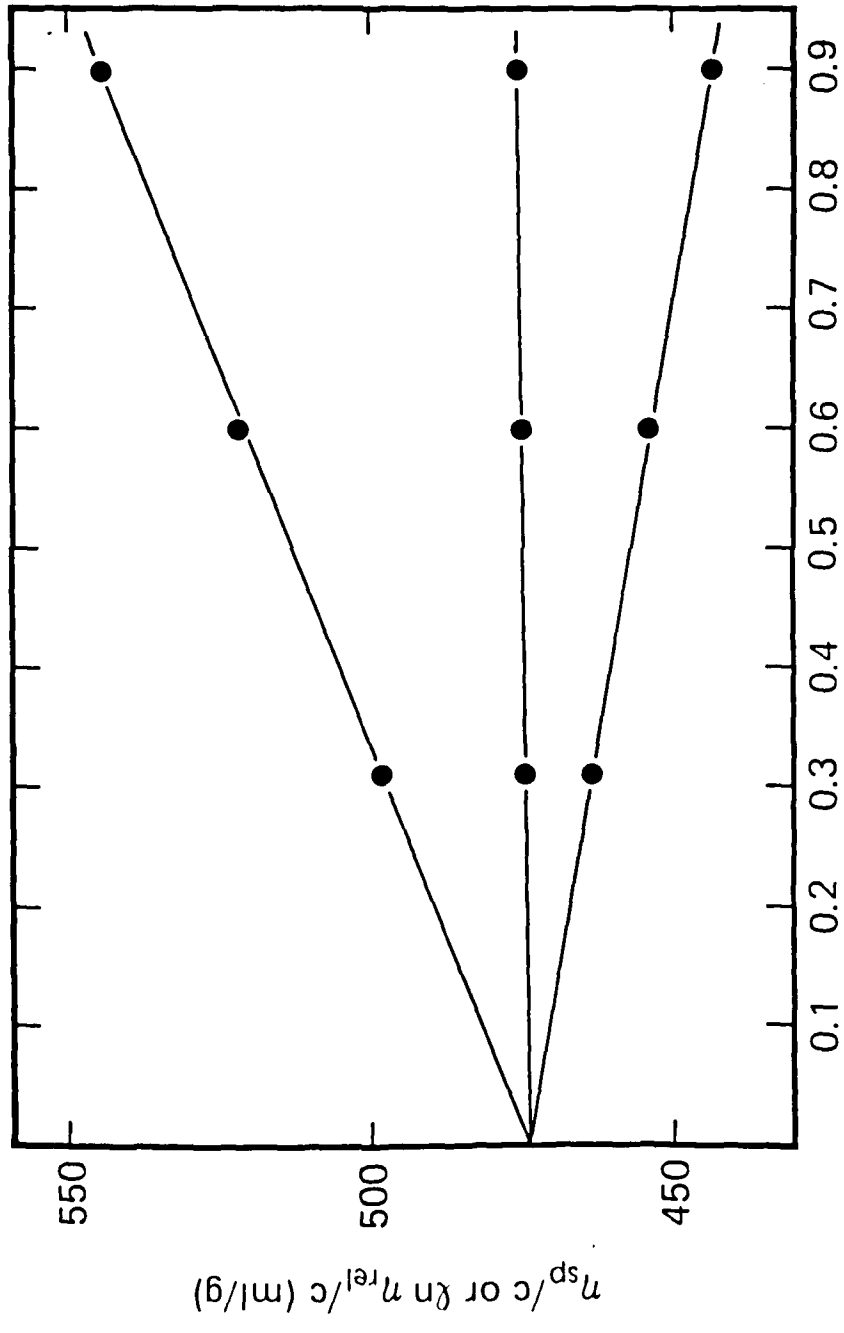

Figure 5. The reduced viscosity, η_{sp}/c, and the inherent viscosity, $\ln \eta_{rel}/c$, as a function of concentration for $(n\text{-hexyl}_2Si)_n$ in hexane at 20°C.

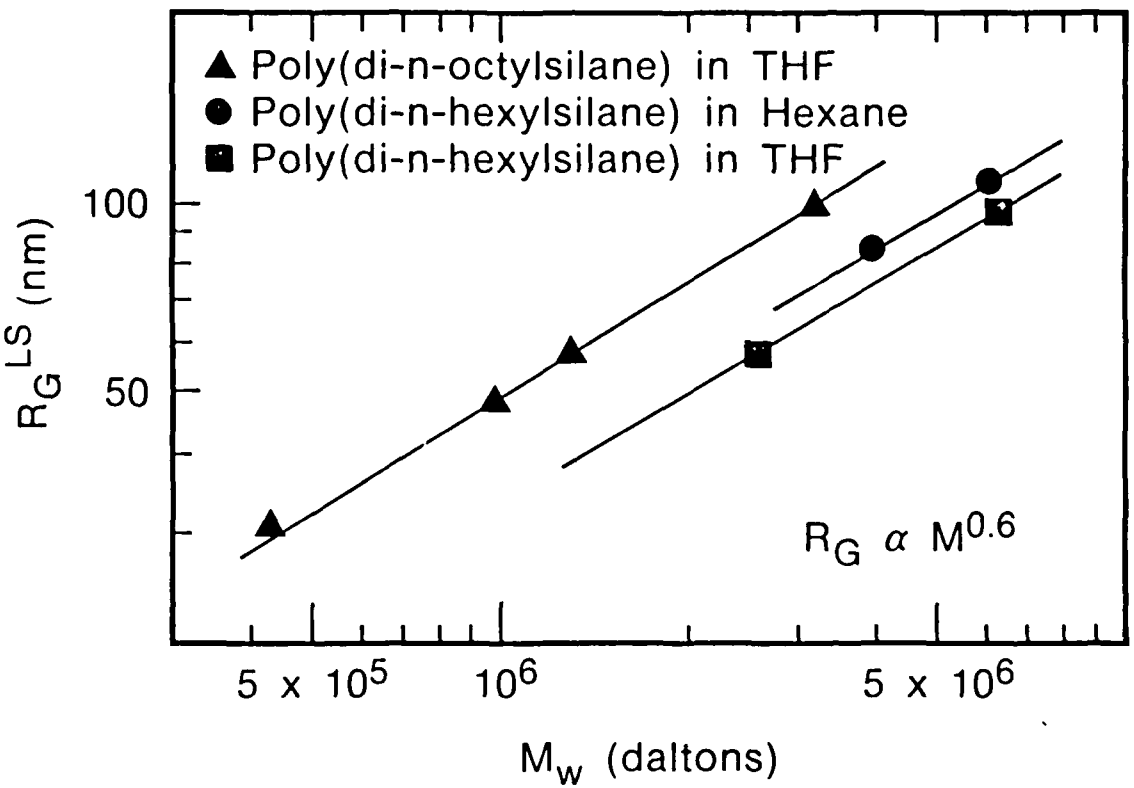

Figure 6. The dependence of the root mean square radius of gyration from light scattering, R_G^{LS}, on M_w for series of $(n\text{-hexyl}_2Si)_n$ and $(n\text{-octyl}_2Si)_n$ obtained by photolytic degradation in THF and hexane.

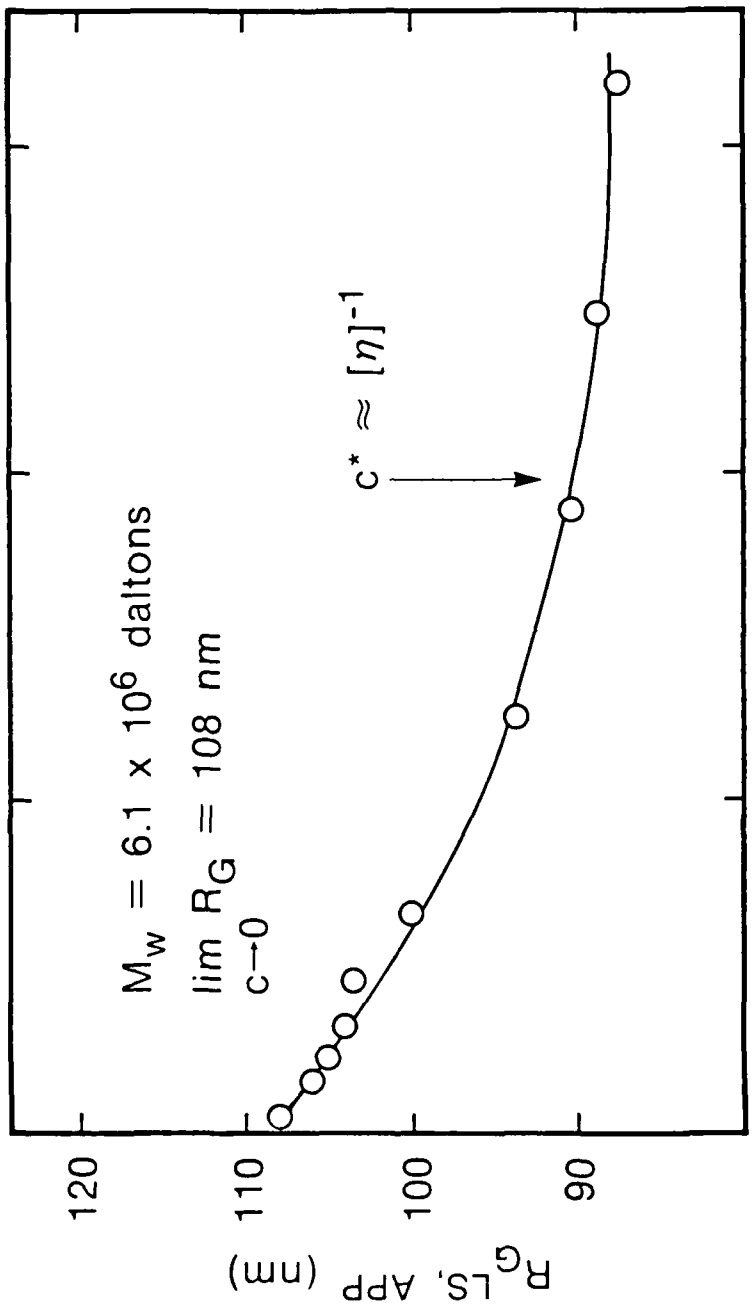

Figure 7. The decrease in $R_G^{LS,APP}$ with concentration for $(n\text{-hexyl}_2Si)_n$ in hexane.

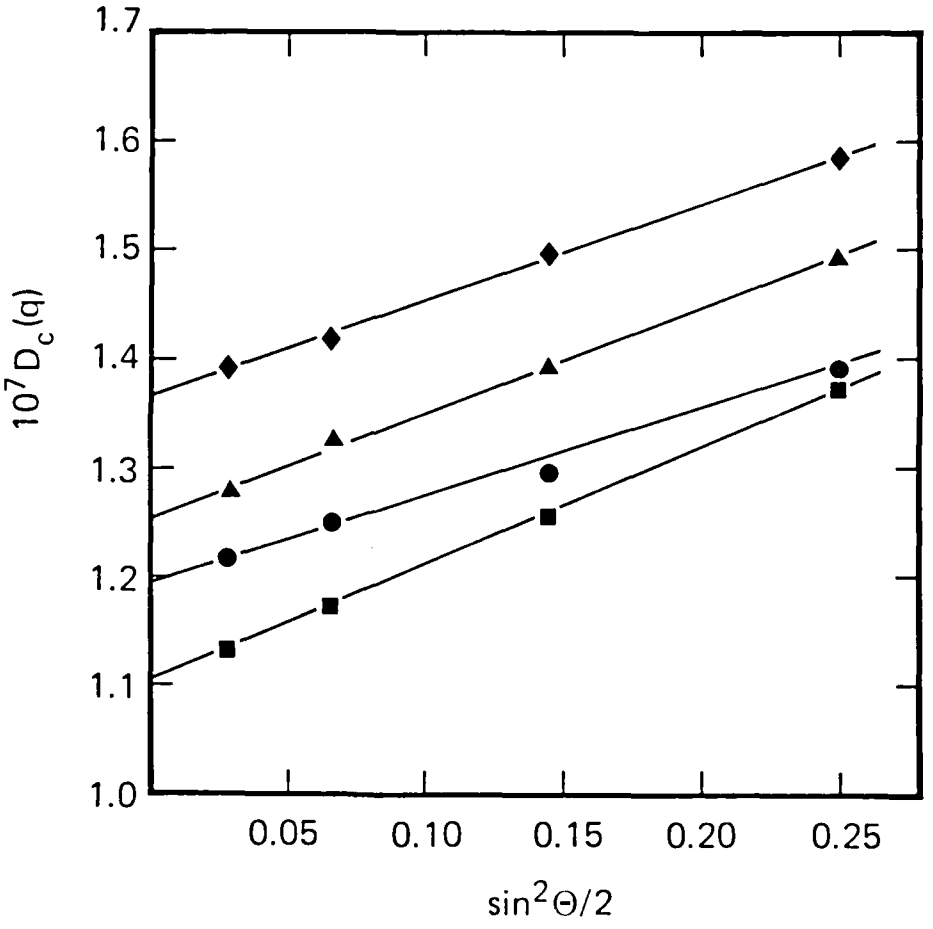

Figure 8. The linewidth Γ obtained from cumulant analysis of dynamic light scattering as a function of scattering angle for four concentrations of $(n\text{-hexyl}_2\text{Si})_n$ in hexane at 25°C.

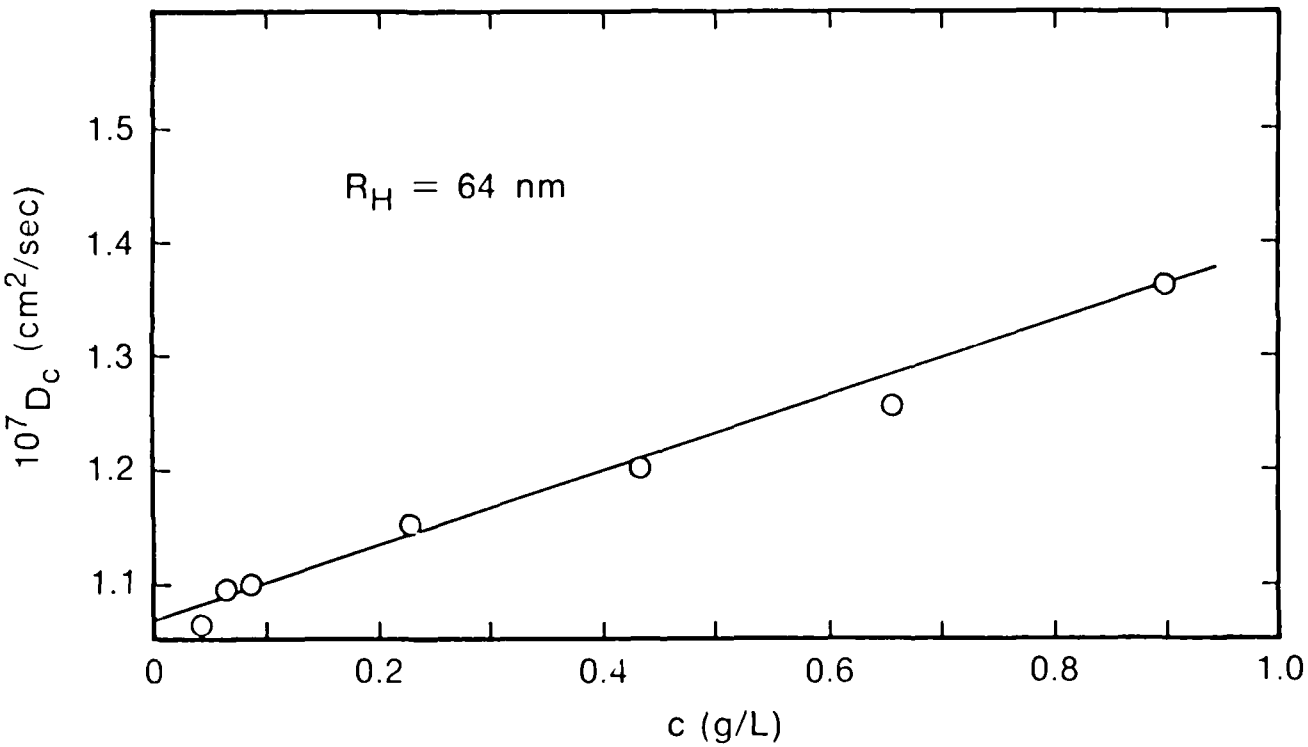

Figure 9. The concentration dependence of Γ_c obtained from extrapolation of Γ to zero angle for $(n\text{-hexyl}_2\text{Si})_n$ in hexane.

END

DTIC

9-86